

The Electrostatic Filopodia Force

Thomas Prevenslik
QED Radiations, Berlin 10777 Germany
thomas@nanoqed.org

Abstract

Classical physics allows the atom to have heat capacity at the nanoscale, the conservation of heat proceeding by an increase in temperature. However, simple QED based on the Planck law of quantum mechanics (QM) denies the atoms in bundles of filament the heat capacity to conserve heat by a change in temperature, the consequence of which is 60-100 nm bundles of 8 nm F-actin filaments protruding from the leading edge of cancer cells conserve thermal heat from the surroundings by producing endogenous simple QED induced EM radiation that at UVC levels charges the filopodia positive by the photoelectric effect. Cancer mitosis occurs as the endogenous UVC continuously charges the filopodia filaments positive thereby providing the electrostatic force that pulls the cancer cell to the negatively charged normal cells, but may stall if the charged filopodia is trapped in the extra cellular matrix. In muscle contraction, simple QED similarly charges the myosin heads, but differs in that the CNS produces action potentials to control charging. Herein, the latest simple QED requirement of a penetration depth in the bundle surface upon absorbing thermal heat is revised to the spontaneous conversion of thermal heat at the bundle surface to standing EM radiation inside the bundle.

Keywords: Cancer, Metastasis, Planck law, Filopodia, Neutrophils, Angiotropism.

1. Introduction

The Cancer Nanoparticle (NP) treatment [1] based on the simple QED induced UVC radiation from ~80 nm lipid NPs induced cancer cell apoptosis while collateral DNA damage to normal cells is corrected by DNA repair systems. Further and independent of NP induced apoptosis of cancer cells, simple QED was shown to emit UV radiation in the filopodia at the leading edge of the cancer cell to cause DNA damage and induce metastasis in nearby normal cells. However, the mechanism by which the UV radiation from filopodia spreads the cancer cell to normal cells was not described.

Cancer is generally thought [2] to spread by the process of intravasation through blood vessel walls allowing the cancer cell to enter the bloodstream and metastasize to distant sites. To penetrate the vessel wall, the cancer cell secretes substances to degrade the basement membrane and extracellular matrix. Once the cancer cell arrives at a distal point in the bloodstream, the cancer cell once again interacts with the endothelial cells by secreting substances to penetrate the vessel wall by the process of extravasation proliferates at new tissue to produce the secondary tumour.

However, the intra and extravasation of cancer cells in penetrating blood vessel walls is difficult and not efficient. In this regard, angiotropism was proposed [3] as an alternative metastasis of cancer cells and extended [4] to Extravascular Migratory Metastasis (EVMM) where cancer cells move along the outside surface of blood vessels by an interaction between the cancer cells and the vessel surface thereby avoiding the difficulty of intra and extravasation through vessel walls.

With EVMM, the cancer cells mimic pericytes on the outside of blood vessels by creeping along the blood vessel until they reach a point to form new tumors. Although not internal cancer, a mouse skin model of melanoma exposed to surface UV radiation was found [5] to accelerate the angiotropic effect leading a dramatic increase in lung metastases. The angiotropic effect was thought to depend on the activation of neutrophils from UV damaged surface keratinocytes that promote inflammation for melanoma cells to migrate towards normal cells. However, the angiotropic effect for internal blood vessels is extremely unlikely to depend on UV damaged at distal keratinocytes in skin.

Neutrophils are cells of the immune system [6] in the extracellular medium that upon activation generate Neutrophil Extracellular Traps (NETs) of fibres that kill bacteria before entering the cell. NETs comprise globular domains of around 25 nm that aggregated into larger fibres with diameters of up to 50 nm. Like filopodia filaments, the neutrophil fibres emit simple QED induced EM radiation that inactivates bacteria before reaching normal cells, but as a bactericide causes inflammation.

In neutrophils, the activation of NET fibres by UVA and UVB radiation was shown [7] much faster than activation by chemical or biological factors. Although UV activation is prompt, the migration of neutrophils decreased within minutes most likely because the NET fibres [6] are no longer bound to the neutrophil body. After 30 minutes, UV irradiated neutrophils [7] lost all ability to migrate. What this means is simple QED induced EM radiation is charging the NET fibres positive, and therefore neutrophils still having attached fibres are attracted to the naturally negative normal cells, and if not attached, only the free NET fibres migrate - not the neutrophils. Contrary to [5], the

UV activated neutrophils do not enhance angiotropism, but the freely suspended NET fibres do provide extracellular antibiotic protection of the cell against pathogens.

With regard to forces driving angiotropism, the force exerted on the filopodia filaments attached to cancer cells measured with optical tweezers was found [8] showed no force is produced in the absence of actin polymerization, the latter defined as the assembly or disassembly of actin filaments by the addition or removal of actin monomers in the filopodia filament. In support of actin polymerization, a polymer bead attached to the tip of a single filament is optically trapped [9] to measure forces, the other end of the filament displaced to produce a pushing force. However, the measured force of a single filament was found to buckle and not be representative of the bundle of filaments in filopodia, perhaps explaining why F-actin filaments rarely exist [10] as isolated single filaments and instead associate into bundles.

In cancer, an overabundance of HER2 molecules in filopodia and lamellipodia was found [11] to activate protrusion growth of filaments that require no active energy sources and diffuse freely within filopodia at the leading edge of migrating tumours. HER2 activation, propagation, and functional protrusion growth is a local process in which filopodia have evolved to exploit Brownian thermal fluctuations within a barrier-free nanostructure to transduce rapid signalling. Filopodia a few microns long with a diameter of about 100 nm are illustrated in Fig. 1.

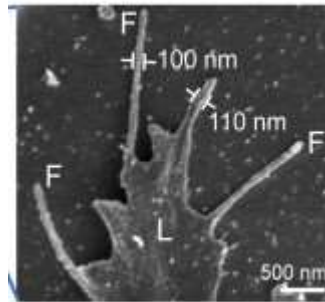


Figure 1. Filopodia (F) at leading edge of Cancer cells (L) lamellipodium

Unlike cancer metastasis by HER2 without an energy source, simple QED requires thermal energy in the surroundings as the source to produce UV radiation within the bundle of filaments in filopodia. The UV can not only activate HER2 to produce the protrusion force of filopodia, but also the energy for UV enhanced ATP dehydration synthesis to grow the filopodia length. With regard to anti-HER2 cancer treatments, psoralen [12] in the inactivation of HER2 by UVA radiation may be extended to the Nanoparticle Treatment [11] at UVC levels.

In simple QED induced UV, the bundle of filaments in filopodia is important - the single filament inconsequential. The typical 60-100 nm bundle [13] having diameter D_b comprises 25-30 filaments (yellow) of 8 nm diameter $D_{f \text{ separated}}$ by fascin cross-linker spacers (blue) shown in Fig. 2.

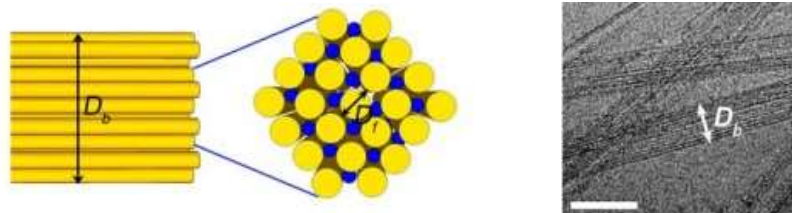


Figure 2. Actin Bundles and Filaments

The micrograph in Fig. 2 shows the side view of the bundle. Scale bar = 200 nm. Although extensively studied in the literature, the filament diameter D_f is observed only as a long molecule inside the bundle. Single filaments are not found *in vivo* as separately distinct, but rather bundled. Nevertheless,

the single F-actin filament *in vitro* is found [14] to have a negative charge density of $q_n = 4 \text{ e/nm}$. In the bundle, simple QED charging produces positive charge density q_p depending on the bundle diameter D_b from which the average net charge q_{net} on the filament is, $q_{net} = q_p - q_n$, the difference between positive and negative charge.

In contrast, the filopodia literature is not focussed on bundles of filaments, but rather on single filament mechanical and chemical models. Beyond mechanical models of buckling, chemical models of the single filament in MD simulations [15] are proposed to explain polymerization and depolymerization by ATP hydrolysis - not ATP synthesis by UV enhanced dehydration [16] in the polymerization cycle of actin as embodied in this paper.

2. Purpose

Cancer spreading between adjacent cells or along the exterior surfaces of blood vessels to distal organs by EVMM requires an external force to move the cancer cell. The purpose of this paper is to assess an electrostatic force based on the production of net positive charge q_{net} in filopodia bundles, a net charge $q_{net} > 0$. In filopodia, at the leading edge of the cancer cell pulled to the naturally charged negative surface of adjacent cells or vessel walls in the direction of movement.

3. Analysis

Filopodia are protrusions of 60-100 nm bundles of actin filaments at the leading edge of cancer cells that by metastasis spread the cancer to normal cells illustrated in [17] and modified by the electrostatic filopodia parameters of simple QED induced EM radiation produced from thermal heat Q in the surroundings is shown in Fig. 3.

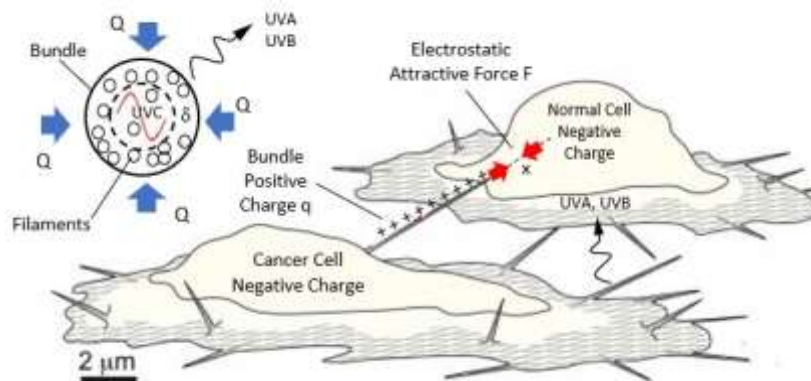


Figure 3. Electrostatic filopodia in metastasis of cancer cells to normal cells.

The simple QED analysis is based on the parameters of the electrostatic filopodia as shown in Fig. 3. A reference diameter d selected as, $d = 70 \text{ nm}$ to describe analysis parameters. Diameters $d < 70 \text{ nm}$ produce ionizing EM radiation in the UVC and beyond that upon absorption is shown to spontaneously create a net positive charge $+q$ producing the electrostatic filopodia force F that translates the cancer cell toward the normal cells. Although less ionizing than UVC radiation, UVA and UVB are produced in bundles having $d > 70 \text{ nm}$ which do not charge the filopodia and are not involved in translational metastasis. Instead, UVA and UVB radiation emitted from the bundle initiates cancer by inducing DNA damage in adjacent normal cells, another form of metastasis.

3.1 Simple QED

Simple QED is a method [1] of nanoscale heat transfer that conserves heat with EM radiation instead of temperature. QED stands for quantum electrodynamics, a complex theory based on *virtual* photons advanced by Feynman and others. In contrast, simple QED is far simpler based on the Planck law that only requires the heat capacity of the atoms in nanostructures to vanish allowing conservation to proceed by the creation of *real* photons comprising EM waves standing across the nanostructure. Like electron orbitals, simple QED quantum states are size dependent based on the dimension of the nanostructure over which the EM waves stand.

By classical physics, the thermal kT heat capacity of the atom is independent of the EM confinement wavelength λ , where k is the Boltzmann constant and T absolute temperature. QM differs as the heat capacity of the atom decreases under EM confinement $\lambda < 100$ microns, and at the nanoscale for $\lambda < 100$ nm, the heat capacity may be said to vanish. The Planck law at 300 K is illustrated in Fig. 4.

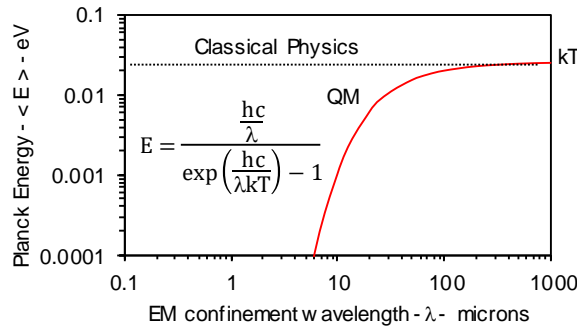


Figure 4. Planck law of the Atom at 300 °K

In the inset, E is Planck energy, h Planck's constant, c light speed, and λ EM wavelength

Unable to conserve the heat Q by a change in temperature, simple QED requires conservation of heat by the creation of EM radiation standing inside and across the bundle diameter d . The time τ to create the standing wave, $\tau = 2(d - 2\delta)/(c/n)$, where the refractive index n of the actin corrects for the velocity c of light in the filament packed bundle. Since $\delta \ll d$, $\tau \sim 2nd/c/n$. Hence, the Planck energy E ,

$$E = h/\tau = hc/2nd$$

having wavelength $\lambda = 2nd$ as noted in Fig. 3 and illustrated in Fig. 5.

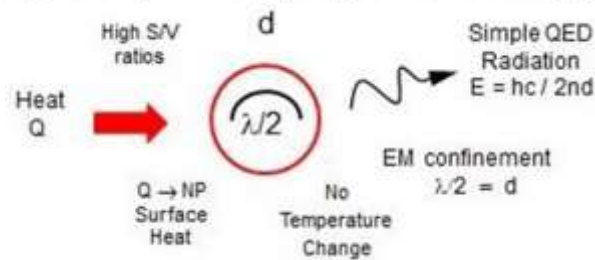


Figure 5. Planck energy of simple QED radiation in a NP

3.2 Penetration Depth

In the bundle, the EM confinement [1] occurred by the high surface-to-volume ratio of nanostructures that requires the thermal heat Q from the surroundings the heat itself as EM energy providing the brief EM confinement necessary to create half waves standing across the internal dimension $2(d - 2\delta) \sim 2d$ of the bundle, where δ is the penetration depth of the heat Q . For heat Q in the far IR having wavelength $\lambda \gg d$, the absorption occurs in the penetration depth δ over the full surface noted in Fig. 3.

In this paper, simple QED is revised to not require a penetration depth δ as the Planck law precludes thermal energy Q in the nanostructure. Instead, simple QED spontaneously converts the heat Q to standing EM waves at the surface of the nanostructure. Unless the nanostructure is absorbent at wavelength $\lambda = 2nd$, the EM wave upon creation is free to be emitted to the surroundings.

3.3 Electrostatic Charge

The number N_p of simple QED photons created in the 70 nm bundle have the same thermal energy U of all atoms in the in the bundle filaments, but not as temperature. Only non-thermal photons are allowed in the bundle as the Planck law precludes temperature at the nanoscale. The thermal energy U of the bundle is,

$$U = 3/2 NKT$$

The volume V of a bundle is $V = \pi d^2 L / 4$ and mass $W = \rho V$. Taking $L = 1$ nm and $d = 70$ nm, $V = 3.85 \times 10^{-24}$ m³. For actin, $\rho = 1148$ kg/m³ and $W = 4.42 \times 10^{-21}$ kg. The atomic weight of actin 536 gives the number of atoms $N = (W / 536) \cdot A_v \sim 5000$. For $T = 300$ K, the heat Q is the thermal energy $U = 3.10 \times 10^{-17}$ J ~ 200 eV/nm.

Simple QED conserves heat Q by creating standing EM radiation across the bundle diameter d having wavelength $\lambda = 2nd$, where n is the index of refraction of the filament actin. Taking DNA as representative of actin, the refractive index $n = 1.5$ at 400 nm [18] is *guessed* as $n \sim 2$ at $\lambda < 100$ nm. Hence, $\lambda \sim 280$ nm in the UVC having Planck energy $E = 4.4$ eV. The number N_p of UV photons created is, $N_p = Q/E = \sim 45$ UVC photons/bundle/nm.

The absorption spectrum for actin proteins (guanine, tryptophan) is taken from tubulin [19] as shown in Fig. 5.

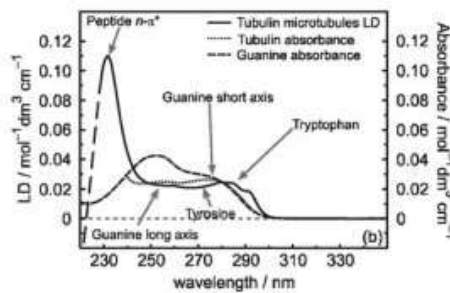


Figure 5. Near-UV absorbance tubulin spectrum

The UVC at 280 nm is absorbent and should produce q positive charge. Recall EUV (< 200 nm), UVC (200 to 280 nm), UVB (280 to 320 nm), and UVA (320 to 400 nm). Unlike UVC, the DNA absorbance vanishes for $\lambda > 300$ nm UVB and UVA radiation is not absorbed and charge q is not produced.

If the absorption of UVC is treated by Beer's law, the UVC may not be absorbed as the required absorption thickness is typically far greater than the nanoscale dimensions of the actin bundle. What this means is the heat Q on the surface of the bundle moving inward as standing EM wave is necessarily absorbed in the bundle before emission to the surroundings, i.e., Beer's law is not applicable as the UVC radiation is not passing through the bundle, but is created in the bundle.

3.4 Electrostatic Force

Analysis of the forces exerted by filopodia has been limited to theoretical considerations, while experimental analysis [8,9,14] has been limited to samples of isolated filaments by optical trapping a bead attached to a filament or a bundle of filaments. Measured forces range from 1 to 2 pN in isolated actin filaments and microtubules to ~ 1 nN in migrating keratocytes. The electrostatic force F between the tip of a positive charged $+q$ filament of length L and a normal cell as a function of the separation x is illustrated in Fig. 6.

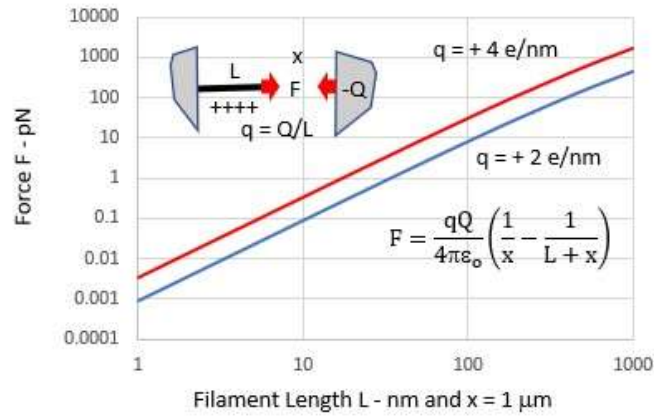


Figure 6. Cancer to normal cell attractive force at 1 μ m separation

In Fig. 6, experiments in support of the electrostatic force F are not available. From Section 3.3, the positive charge density of $q = +2 \text{ e/nm}$ for a single filament of length L interacting with a negative charged normal cell assumed to have negative charge $Q = -q \cdot L$ at distance $x = 1 \mu\text{m}$ shows the force F of 1 - 2 pN is reached for $x = 1 \mu\text{m}$ at linear charge at $L \sim 60 \text{ nm}$. For the same $x = 1 \mu\text{m}$, the force F increases with L reaching the $\sim \text{nN}$ level at $L \sim 1.2 \mu\text{m}$. From [14] with $q = 4 \text{ e/nm}$, the force F is higher and similar.

4. Discussion

4.1 Charge density

In biophysics, it is well established [20] that like-charged macromolecules can aggregate under the influence of oppositely charged divalent ions, e.g., actin as an anionic rod-like polymer having a negative charge density $q_n = 4 \text{ e/nm}$. Unlike simple QED that creates positive charge, a linear distribution of positive counterions per unit length is assumed to allow like-charge attraction.

Calculated charge density [21] of 1.65×10^5 and $1.2 \times 10^5 \text{ e}/\mu\text{m}$ have been reported, although the number of filaments in an actin bundle are not clear. In this paper, the simple QED analysis of the 70 nm diameter bundle of 25 filaments absent counterions produced $0.45 \times 10^5 \text{ UVC photons}/\mu\text{m}$ or 45 UVC photons/nm.

Since each UVC photon produces 1 positive charge, and since about 25 filaments are included in typical bundle, about $q_p = 45 \text{ e}/25 \sim 2 \text{ e/nm}$ which is actually less than the intrinsic negative charge of $q_n \sim 4 \text{ e/nm}$ predicted [14] for a single actin filament. What this means is the net q_n charge, $q_{\text{net}} = q_p - q_n < 0$ and the attractive force between filaments does not occur. Instead, the filament overall is negatively charged. The q_p charge is therefore localized heterogeneously at discrete atoms along the actin filament length [22] as illustrated in Fig. 7.

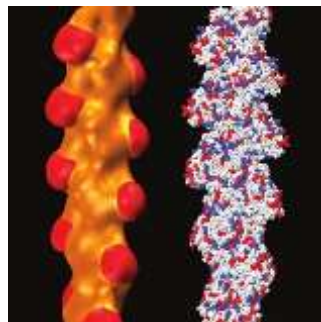


Figure 7. Heterogeneous charge distribution in actin filaments

Fig. 7 on the right is a high-resolution representation of F-actin. The interpretation [22] is negatively charged residues (red) and positive charged residues (blue) are small fractions of neutral residues (white). However, simple QED requires the dominant negative charged residue to neutralize the smaller UVC induced positive charge. Shown on the left is a low-resolution density actin map. The protrusions (red) are the highly negative charge regions thought to significantly modulate the positive counterion distribution. More study is suggested.

In contrast, the simple QED positive charges $q_p = 2 \text{ e/nm}$ are insufficient to at least neutralize the filament by making the net charge $q_{\text{net}} \sim 0$. Alternatively, neutrality in the assembly of filaments to a bundle requires the net charge $q_{\text{net}} = 4 \text{ e/nm}$.

4.2 Ambient thermal heat Q cycles

The heat Q in creating the positive charge q_p was assumed be the thermal U energy of the atoms that otherwise would have occupied the bundle at the temperature T of the surroundings. But once the heat Q is converted to 45 UVC photons/nm, the thermal energy U is regained to allow the cycle to repeat by generating an additional 45 UVC photons/nm, and so on *ad infinitum*. Hence, the net charge q_{net} on the bundle continually increases until neutralized as the filopodia tip contacts the normal cell.

What this means is only 2 conversions of heat Q to 45 UVC photons/nm are necessary to neutralize the 25 filaments in the bundle, the next Q conversion producing a net charge/filament $q_{\text{net}} = 3 \times 2 - 4 = 2 \text{ e/nm} > 0$ to provide an attractive force between the cancer and normal cells. Similarly, the assembly of filaments into a bundle only requires 2 conversions of heat Q into UVC photon achieve neutrality. Positive counter ions between adjacent filaments to offset natural acting negative charge are not necessary.

4.3 Muscle Contraction

Cancer mitosis by the simple QED continuous positive charging of filopodia is interrupted by neutralization upon contact with negatively charged extracellular matrix prior to eventually contacting normal cells. Similarity is found [23] in muscle contraction by the positive + charging of myosin and heads pulling the negative charged α -actin in the Z-disks together as shown in Fig. 8.

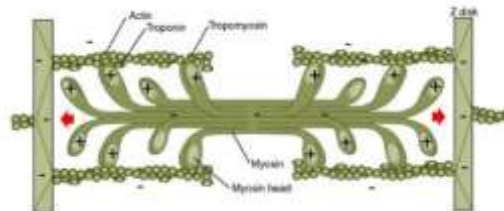


Figure 8. Electrostatic Muscle contraction

Muscle contraction is far more efficient than cancer mitosis not only because of the absence of the extracellular matrix, but more importantly as action potentials from the CNS are applied at the Z-disks that control when the muscle contraction begins. But like the filopodia filaments, simple QED is constantly charging positive the myosin and heads provided they are not in contact with the negative charged actin. The sequence in muscle contraction is shown in Fig. 9.

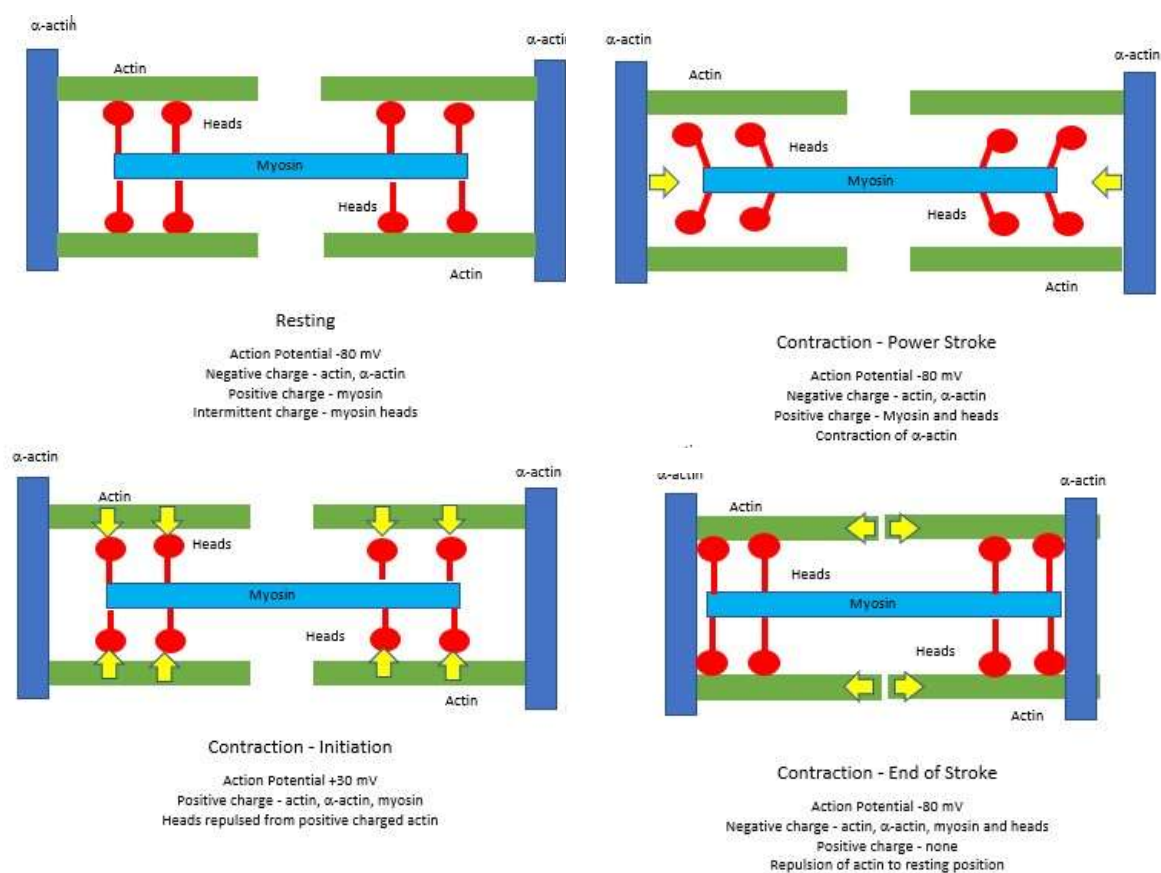


Figure 9. Muscle contraction controlled by Action Potentials

Fig. 9 shows the driving mechanism in muscle contraction is the persistent creation of simple QED radiation to charge the myosin and heads positive while the surroundings actin and α -actin remain negatively charged except during the momentary positive action potential. In muscle contraction, the myosin heads when not in contact with actin charge positive and during contact are acquire a negative charge. Only at the end of the power stroke as the myosin tip collides with the α -actin Z-disk do the myosin and heads acquire a negative charge of actin. Repulsion of the like-charged myosin and heads from the α -actin returns the muscle to the resting position

5. Conclusions

Metastasis of cancer by simple QED induced UVC emission produces positively charged filopodial bundles of filaments that electrostatically attract that the cancer to the negative charged normal cells including diversions to the extracellular matrix.

In bundles of 25 filaments, filopodia tips separated by 1 μm from a cancer cell in a filopodia having a net positive charge of +2 e/ nm produce electrostatic attractive force $F > 2$ pN for filament lengths > 100 nm.

In EVMM with cancer cells moving along the outside surface of blood vessels, the electrostatic attraction to the vessel wall is on the order of 2 pN/ μm .

Single filament filopodia not observed *in vivo* are only of academic interest. Instead, bundles of ~25 actin filaments should be the focus in cancer metastasis.

Simple QED creates UVC radiation producing positive charge in the filopodia bundles is a continuous process supplied by cycles of heating from the thermal surroundings until the tip contacts negatively charged normal cells or the extracellular matrix.

Single actin filaments are not positively charged because the number of atoms in a filament is insufficient to produce UVC radiation and is consistent with the long-standing notion of counterions to avoid like-charge repulsion and achieve neutrality in the assembly of filaments into bundles.

Unlike single filaments, assembly of 25 - 30 filaments having far more atoms produce UVC to allow assembly without the need of counterions to avoid like-charged repulsion, a notion that may be extended to actin polymerization thought to be a precursor to filopodia producing force.

The long-standing notion in biophysics that like-charged macromolecules can aggregate under the influence of oppositely charged counterions needs revision for larger numbers of macromolecules.

Single actin filaments thought to require counterions to avoid the like-like repulsion in assembly is not necessary as the number of atoms in a single filament simple QED induced positive charges cannot produce are produced bundles of 25 - 30 filaments.

Stalling of filopodia growth occurs as the bundle of filaments contact negatively charged extra cellular matrix fibers.

Neutrophil fibres having diameters ~50 nm emit simple QED induced EM radiation do indeed act as a bactericide to inactivate bacteria before reaching normal cells.

Simple QED of filopodia in cancer metastasis finds similarity with myosin bundles in muscle contraction. The basic difference is the direction of the electrostatic force from charging of myosin is well defined and controlled by action potentials from the CNS; whereas, the filopodia in cancer metastasis grow depending on the random directions of electrostatic attraction to negatively charged normal cells or the extracellular matrix.

References

1. Prevenslik T. (2020) Cancer: UVC in the Nanoparticle Treatment and Metastasis. See nanoqed.org, 2020.
2. Martin T. A., et al. (2013) Cancer Invasion and Metastasis: Molecular and Cellular Perspective. *Metastatic Cancer: Clinical and Biological Perspectives* edited by Rahul Jandial ©2013 Landes Bioscience.
3. Barnhill, R., Lugassy, C. (2004) Angiotropic malignant melanoma and extravascular migratory metastasis: description of 36 cases with emphasis on a new mechanism of tumour spread. *Pathology* 36:485–490.
4. Lugassy C., Barnhill R. (2014) Ultraviolet-radiation-induced inflammation promotes angiotropism and metastasis in melanoma. <https://www.uclahealth.org/u-magazine/uv-light-aids-creeping-cancer-cells>
5. Bald T., et al. (2014) Ultraviolet-radiation-induced inflammation promotes angiotropism and metastasis in melanoma. *Nature* 507:109–113.
6. Brinkman V., et al. (2004) Neutrophil Extracellular Traps Kill Bacteria. *Science* 303:1532. DOI: 10.1126/science.1092385.
7. Zawrotniak M., et al. (2019) UVA and UVB radiation induce the formation of neutrophil extracellular traps by human polymorphonuclear cells. *Journal of Photochemistry & Photobiology B: Biology* 196:111511
8. Cojoc D., et al. (2007) Properties of the Force Exerted by Filopodia and Lamellipodia and the Involvement of Cytoskeletal Components. <https://journals.plos.org/plosone/article?id=10.1371/journal.pone.0001072>
9. Footer M.J., et al. (2007) Direct measurement of force generation by actin filament polymerization using an optical trap. *PNAS*: 2181–2186.

10. Haviv L., et al. (2008) Thickness distribution of actin bundles in vitro. *Eur Biophys J.*, 37:447–454.
11. Lam W. Y., et al., (2019) HER2 Cancer Protrusion Growth Signalling Regulated by Unhindered, Localized Filopodial Dynamics. *bioRxiv* <https://doi.org/10.1101/654988>.
12. Oldham M., et al. (2016) X-Ray Psoralen Activated Cancer Therapy (X-PACT). *PLoS ONE*, 11: e0162078. doi:10.1371/journal.pone.0162078.
13. Haviv L., et al. (2008) Thickness distribution of actin bundles in vitro. *Eur Biophys J* 37:447–454.
14. Angelini T. E., et al. (2003) Like-charge attraction between polyelectrolytes induced by counterion charge density waves. *PNAS* 100: 8634–8637
15. Prevenslik T. (2019) ATP Synthesis by Endogenous UV Radiation. 10th Targeting Mitochondria Congress, October 27-29, 2019
16. Splettstoesser T., et al. (2011) Structural modeling and molecular dynamics simulation of the actin filament. *Proteins*, 79:2033–2043.
17. Bornscholgl T. (2013) How filopodia pull: What we know about the Mechanics and Dynamics of Filopodia. *Cytoskeleton*, 70:590-603.
18. Jung W., et al, (2017) Cationic lipid binding control in DNA based biopolymer and its impacts on optical and thermo-optic properties of thin solid films. *Optical Materials Express* 7: 3796.
19. Bulheller B. M., et al. (2007) Circular and linear dichroism of proteins. *Phys. Chem. Chem. Phys.*, 7:2020–2035.
20. Sanders L. K., et al. (2007) Control of electrostatic interactions between F-actin and genetically modified lysozyme in aqueous media. *Proc Natl Acad Sci USA.* 104:15994–15999.
21. Cantiello H. C., et al. (1991) Osmotically induced electrical signals from actin filaments. *Biophysical Journal* 59:1284-1289.
22. Angelini T. E., et al. (2006) Counterions between charged polymers exhibit liquid-like organization and dynamics. *PNAS* 103: 7962–7967.
23. Prevenslik T. (2020) Electrostatic Muscle Contraction. See nanoqed.org, 2020.